



## Observation of Coherence in the Time-Reversed Relativistic Photoelectric Effect

S. Tashenov,<sup>1</sup> D. Banaś,<sup>2</sup> H. Beyer,<sup>3</sup> C. Brandau,<sup>4,5</sup> S. Fritzsche,<sup>6,7</sup> A. Gumberidze,<sup>4,5</sup> S. Hagmann,<sup>3</sup> P.-M. Hillenbrand,<sup>3</sup> H. Jörg,<sup>1</sup> I. Kojouharov,<sup>3</sup> Ch. Kozhuharov,<sup>3</sup> M. Lestinsky,<sup>3</sup> Yu. A. Litvinov,<sup>1,3</sup> A. V. Maiorova,<sup>8</sup> H. Schaffner,<sup>3</sup> V. M. Shabaev,<sup>8</sup> U. Spillmann,<sup>3</sup> Th. Stöhlker,<sup>6,9</sup> A. Surzhykov,<sup>6</sup> and S. Trotsenko<sup>3,6</sup>

<sup>1</sup>Physikalisches Institut der Universität Heidelberg, 69120 Heidelberg, Germany

<sup>2</sup>Institute of Physics, Jan Kochanowski University, 25-406 Kielce, Poland

<sup>3</sup>GSI Helmholtzzentrum für Schwerionenforschung GmbH, 64291 Darmstadt, Germany

<sup>4</sup>ExtreMe Matter Institute EMMI and Research Division, GSI Helmholtzzentrum für Schwerionenforschung, 64291 Darmstadt, Germany

<sup>5</sup>FIAS Frankfurt Institute for Advanced Studies, 60438 Frankfurt am Main, Germany

<sup>6</sup>Helmholtz-Institut Jena, 07743 Jena, Germany

<sup>7</sup>Theoretisch-Physikalisches Institut, Friedrich-Schiller-Universität Jena, 07743 Jena, Germany

<sup>8</sup>St. Petersburg State University, 198504 St. Petersburg, Russia

<sup>9</sup>Institut für Optik und Quantenelektronik, Friedrich-Schiller-Universität Jena, 07743 Jena, Germany

(Received 29 June 2014; published 9 September 2014)

The photoelectric effect has been studied in the regime of hard x rays and strong Coulomb fields via its time-reversed process of radiative recombination (RR). In the experiment, the relativistic electrons recombined into the  $2p_{3/2}$  excited state of hydrogenlike uranium ions, and both the RR x rays and the subsequently emitted characteristic x rays were detected in coincidence. This allowed us to observe the coherence between the magnetic substates in a highly charged ion and to identify the contribution of the spin-orbit interaction to the RR process.

DOI: 10.1103/PhysRevLett.113.113001

PACS numbers: 32.80.Fb, 12.20.Ds, 32.80.Qk, 34.80.Lx

The photoelectric effect is one of the fundamental and dominant atomic processes in which matter absorbs electromagnetic radiation in the energy range from visible light to hard x rays. It led to the development of quantum mechanics [1] and, since then, helped to improve our understanding of light-matter interactions significantly. In these developments, the experiments addressing polarization and alignment properties of the process played a crucial role. In particular, the quantum mechanically complete information about the photoionization was obtained in a number of experiments done in the optical and soft x-ray regimes [2,3].

In contrast to the well-explored optical and soft x-ray regimes, only a few experiments were done in the regime of hard x rays and strong Coulomb fields. The main reason for this was a limited availability of intense sources of polarized hard x rays and the electron straggling in typically used solid targets [4–6]. These limitations were removed by studying the photoelectric effect via its time-reversed process of radiative recombination (RR) of initially free or weakly bound electrons into heavy highly charged ions (HCIs). One experimental approach exploits the properties of the emitted RR x rays, such as their angular distribution with respect to the propagation

direction of the incoming electron [7,8] and their linear polarization [9]. For example, the latter experiment studied, in time reverse, the angular distribution of the electrons photoionized by linearly polarized x rays. It identified that at high energies a significant fraction of the photoelectrons is emitted perpendicular to the x-ray polarization plane. This phenomenon is in stark contrast to the low energy photoeffect. In a complementary approach, the RR x rays are not observed, but the characteristic bound-bound x rays, subsequent to the RR into an excited state, are detected. The RR into the  $2p_{3/2}$  excited state of hydrogenlike uranium, which decays by emission of  $\text{Ly}\alpha_1$  x rays, is a prominent example of such studies [10,11]. Since the RR x rays are not observed, the  $2p_{3/2}$  state is axially symmetric around the propagation direction of the incoming electron, and its magnetic substates are populated incoherently [12]. The electron propagation direction is used as a quantization axis. The population distribution of the magnetic substates is described by the alignment parameter  $\mathcal{A}_{20}$ . The latter is accessed experimentally by the analysis of the angular distribution of the emitted x rays [10,11] and/or their linear polarization [13]. Apart from RR, this approach was used to study the alignment for a number of other collision processes, such as the electron and the nucleus impact excitation [14–18], resonant transfer and excitation [19], and dielectronic recombination [20]. It was shown to be highly sensitive to relativistic effects, for instance, to those caused by the Breit interaction [20,21].

Published by the American Physical Society under the terms of the Creative Commons Attribution 3.0 License. Further distribution of this work must maintain attribution to the author(s) and the published article's title, journal citation, and DOI.

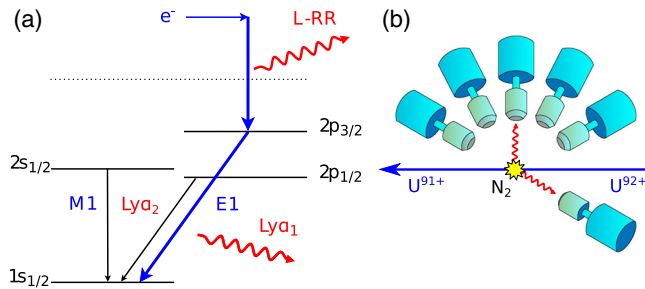


FIG. 1 (color online). The scheme of the experiment: (a) measurement of the correlated  $L$ -shell RR and  $Ly\alpha_1$  x rays emitted in the radiative recombination of the electron into the initially bare uranium ion; (b) the setup of the germanium detectors that registered correlated x rays emitted in collisions of the stored bare uranium beam with the  $N_2$  gas jet.

It was predicted that significantly higher sensitivity to the subtle details of the recombination process can be obtained when both of these x rays emitted by a single ion are detected in time coincidence [22,23], see Fig. 1. In this new type of experiment, the axial symmetry of the RR-populated  $2p_{3/2}$  state is removed, and the reaction plane is defined by the propagation directions of the incoming electron and the emitted RR x ray. In this case, the magnetic substates are populated coherently [24–26]. As a consequence, the state should attain a new alignment axis, which is confined to the reaction plane and forms a finite angle  $\gamma$  with respect to the collision axis [24–26]. This alignment angle  $\gamma$  can be measured via the angular distribution of the  $Ly\alpha_1$  x rays [12,24–28]. So far, the effects of the coherent population of atomic sublevels were never addressed in experiments with HCIs.

In this Letter, we report on the experiment where an electron is captured by a bare ion,  $U^{92+}$ , into the  $2p_{3/2}$  state and both the RR and the  $Ly\alpha_1$  x rays are detected in time coincidence, see Fig. 1. The coincident registration of the x rays completely removes one major restriction of most of the earlier experiments—the contribution of cascades to the alignment of the excited state [10,14–17]. We observed large alignment angles that manifest the coherent population of the magnetic substates. The alignment angles deviate significantly from the predictions of the nonrelativistic calculations but can be explained within our full-order relativistic theory. In a semiclassical picture, this deviation indicates the effect of the spin-orbit interaction in RR.

The measurement was conducted at the experimental storage ring (ESR) of the GSI accelerator complex in Darmstadt [7,8,29]. Typically,  $10^7$  fully ionized uranium ions of the spinless isotope  $^{238}U^{92+}$  were injected into the ring with a kinetic energy of 230 MeV/u. The momentum spread and the lateral extent of the circulating ion beam are minimized employing electron cooling. Electron cooling also guarantees well defined and repeatable conditions throughout the experiment and counteracts energy loss and straggling in the target. A supersonic nitrogen gas jet, with the areal

density of  $10^{13}$  particles/cm<sup>2</sup>, was used as an effective target of unpolarized electrons. The electrons, initially bound in the  $N_2$  molecules, were captured by uranium ions via the radiative electron capture process. For the very asymmetric collision system ( $U^{92+} \rightarrow N_2$ ) and the high beam energy, used in the experiment, the target electrons can be considered to be quasifree and the process to be identical to RR [30]. Furthermore, at this energy the cross section for the competing nonradiative electron capture process is negligible compared to that of RR [30,31]. Details about beam preparation, the experimental environment at the ESR, as well as the gas-jet target, can be found in Refs. [7,8].

The emitted x rays were registered by an array of large polarization-insensitive germanium detectors that observed the target in the horizontal plane at different angles with respect to the beam propagation direction; see Fig. 1(b). The total solid angle coverage was 1%. This is an order of magnitude increase as compared to a typical x-ray detection setup used at the gas-jet target in earlier experiments [7,8]. Correspondingly, the x-ray coincidence efficiency increases by 2 orders of magnitude. To compensate for the large Doppler broadening, associated with the relativistic beam velocity, and the large spread in the x-ray emission angle covered by each detector, we used the segmented detectors such as clover [32], segmented clover [33], and Euroball cluster [34] germanium detectors. Each detector segment was read out by a 100 MHz sampling analog-to-digital converter. The x-ray energies and the arrival times were extracted using digital pulse shape processing [35]. A typical energy resolution of 1–2 keV and a timing resolution of better than 200 ns were obtained. Where the segmentation was not sufficient to compensate for the Doppler broadening and resolve the  $Ly\alpha$  doublet, we achieved this by employing vertical slit x-ray absorbers. Note that the width of the broader RR lines stems from the momentum distribution of the bound  $N_2$  target electrons, i.e., the Compton profile [30].

Uranium ions that captured an electron in the collision with the target, were separated from the stored primary beam in the first dipole magnet downstream from the target and registered by a multiwire proportional counter. Time coincidences of these recombined ions with the emitted x rays suppressed most of the bremsstrahlung continuum that predominantly occurs in electron-ion collisions without a change of the ion's charge state. A typical x-ray spectrum is shown in Fig. 2. The RR into  $K$ ,  $L$ , and higher atomic shells are dominant at high energies, whereas  $Ly\alpha_1$  and  $Ly\alpha_2$  are well pronounced at lower energies.

X-ray cascades consisting of an RR photon (free-bound transition) into excited states of the uranium ion and a subsequent characteristic bound-bound x ray were registered in two separate x-ray detectors in time coincidence. All low-lying excited states of hydrogenlike uranium have lifetimes much shorter than the time resolution of the used x-ray detectors; in particular the lifetime of the  $2p_{3/2}$  state is about  $10^{-16}$  sec. In our analysis, we focused on  $L$ -RR

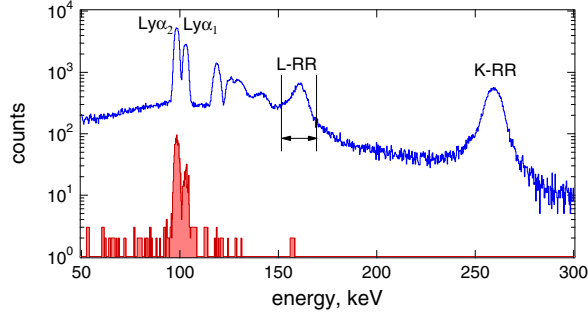


FIG. 2 (color online). Solid line: typical x-ray spectrum Doppler corrected to the ion's rest frame. Filled area: typical x-ray spectrum collected in time coincidence with another x-ray detector that registered an  $L$ -shell RR x ray. The corresponding energy interval is shown.

and the corresponding following  $Ly\alpha$  x rays. Figure 2 shows the window condition on the energy used to select the  $L$ -RR and the resulting promptly emitted  $Ly\alpha$  x ray; see Fig. 1(a). The very low background level in the time-and-energy coincidence spectrum demonstrates clean observation of the correlated x rays emitted by a single heavy ion. Moreover, the coincident x-ray detection suppressed the contribution of the cascades from the  $n > 2$  states to the  $Ly\alpha$  x rays. In earlier alignment experiments, these cascades significantly influenced the results [10,14–17]. In Fig. 3, for each emission direction of the RR x ray, the corresponding

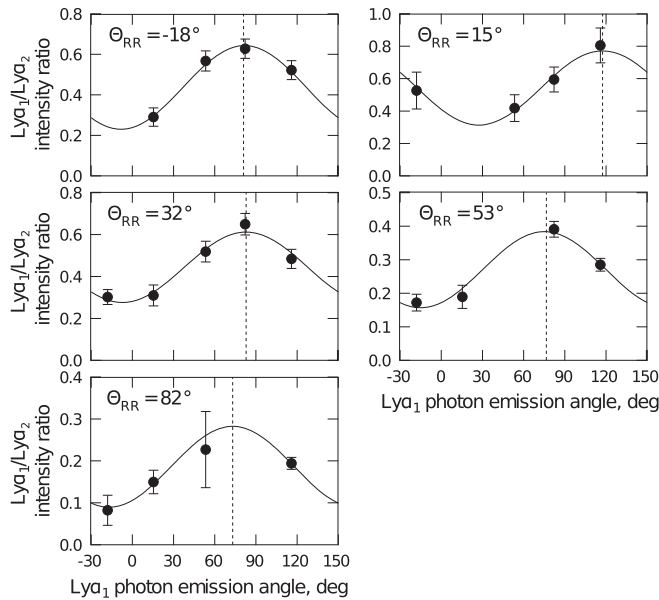


FIG. 3. Intensities of the  $Ly\alpha_1$  x rays measured in coincidence with the  $L$ -shell RR x rays emitted under an angle  $\theta_{RR}$  and normalized on the corresponding intensities of the  $Ly\alpha_2$  isotropic line (symbols). The angles are in the rest frame of the ion relative to the electron propagation direction. The solid lines are the fits of Eq. (2) to the experimental data points. The dashed lines indicate the maxima of the angular distributions.

angular distribution of the coincident  $Ly\alpha_1$  x rays is plotted. To compensate for the solid angle differences between the individual detectors, the intensity of the  $Ly\alpha_1$  line was normalized to the intensity of the isotropic  $Ly\alpha_2$  line.

In order to interpret the observed angular correlations, we employ the quantum-mechanical description of the RR-populated state within the density matrix formalism [12,28]. The density matrix of the  $2p_{3/2}$  state has  $4 \times 4$  individual elements that contain all physically significant information on this state. The diagonal elements give probabilities to find the ion in the corresponding magnetic substates. In order to define the latter, the electron propagation direction in the ion rest frame is taken as the quantization axis. The off-diagonal elements of the density matrix describe the coherence between the magnetic substates [12,28]. When the polarizations of the electron and the RR x ray are not observed, the density matrix is fully defined by three alignment parameters  $\mathcal{A}_{20}$ ,  $\mathcal{A}_{21}$ , and  $\mathcal{A}_{22}$  [22,23], also called the state multipoles [12,24–28]. The alignment parameter  $\mathcal{A}_{20}$  determines all the diagonal elements of the density matrix. The other two alignment parameters  $\mathcal{A}_{21}$  and  $\mathcal{A}_{22}$  define all the off-diagonal elements and, thus, the coherence of the populated state.

The angular distribution of the  $Ly\alpha_1$  x rays depends strongly on the alignment of the populated state. When the RR x ray is not observed, as was the case in all previous alignment experiments with heavy ions, the populated  $2p_{3/2}$  state is axially symmetric and, therefore, its density matrix is diagonal, i.e.,  $\mathcal{A}_{21} = \mathcal{A}_{22} = 0$ . The angular distribution of the  $Ly\alpha_1$  x rays in these experiments was symmetric with respect to the collision axis [10,11]. In contrast, in the present experiment, the alignment parameters  $\mathcal{A}_{21}$  and  $\mathcal{A}_{22}$  are nonzero and the magnetic substates are populated coherently. Therefore, the populated state loses its symmetry with respect to the quantization axis. Figure 4 shows the effect of the coherence on the electric

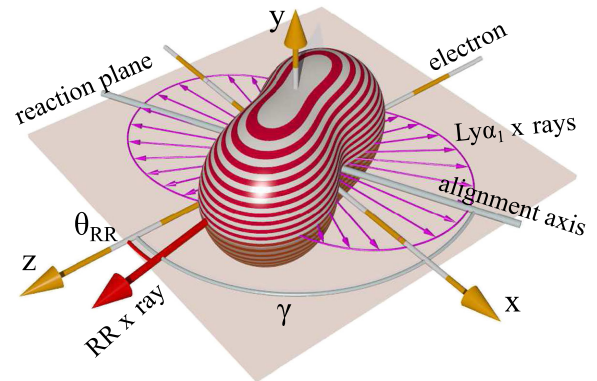


FIG. 4 (color online). The angular density distribution of the charge cloud of the RR-populated  $2p_{3/2}$  state. The quantization axis  $Z$  coincides with the electron propagation direction. Together with the RR x-ray emission direction they define the reaction plane. The latter confines the alignment axis. The emitted  $Ly\alpha_1$  x rays were detected within the reaction plane.

charge density distribution of the populated state [12,27]. The charge cloud has two principal axes: one within the reaction plane; it is called the alignment axis. The second one is perpendicular to the reaction plane; it defines the orientation of the excited state. Note that, in a general case, the charge cloud is not symmetric around the alignment axis. Therefore, the density matrix can not be diagonalized by choosing the alignment axis as the quantization axis. The orientation was not measured in this experiment, and in the following, we focus on the alignment. The alignment axis forms an angle  $\gamma$  with respect to the electron propagation direction [12,24–28]

$$\tan(2\gamma) = \frac{2A_{21}}{A_{22} - \sqrt{\frac{3}{2}}A_{20}}. \quad (1)$$

Here, we call it the alignment angle of the charge cloud. Thus, the nonzero alignment angle is a signature of the coherence between the magnetic substates. It is probed by measurement of the angular distribution of the  $\text{Ly}\alpha_1$  x rays emitted within the reaction plane [22]

$$W(\theta) = A + B \cos 2(\theta - \gamma). \quad (2)$$

The experimental data for each RR emission direction were fitted to this function by treating  $A$ ,  $B$ , and  $\gamma$  as free parameters; the fitted solid lines are shown in Fig. 3.

From Fig. 3, it is evident that the symmetry axes of the angular distributions of the  $\text{Ly}\alpha_1$  x rays do not coincide with the collision axis. We interpret this as a result of an interference of the electromagnetic waves emitted in the decays of the individual magnetic substates. Because of the coherence between the magnetic substates, the corresponding waves attain certain relative phases. This modifies the angular distribution of the emitted radiation.

The measured alignment angle  $\gamma$ , shown in Fig. 5, depends strongly on the RR x-ray emission direction. The predictions of the full-order relativistic theory (solid line) are in perfect agreement with the experiment. In this theory, the electron, both in continuum and bound states, is described by the relativistic Dirac wave functions and all higher (nondipole) terms in the expansion of the electron-photon interaction are taken into account. In comparison to the results of this theory in the nonrelativistic limit, where the electron-photon interaction is restricted to the electric dipole term and the electron wave functions are approximated by the Schrödinger solutions [36], one can derive

$$\gamma = 180^\circ - \theta_{\text{RR}}, \quad (3)$$

which is shown as a dashed line in Fig. 5. The dotted lines indicate the possible alignment angles corresponding to the incoherent population of the magnetic substates.

In the following, we give a simple semiclassical non-relativistic picture of the process. Semiclassically, the alignment parameters  $\mathcal{A}_{2q}$  describe the spacial anisotropy of the total angular momentum vector [12]. In the

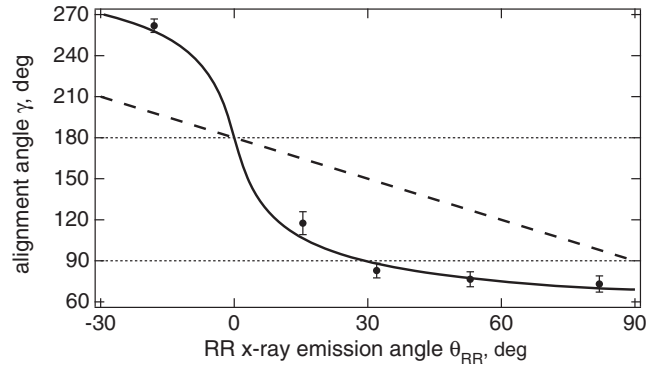


FIG. 5. The alignment angle  $\gamma$  as a function of the RR x-ray emission angle  $\theta_{\text{RR}}$  relative to the electron propagation direction in the rest frame of the ion. The data points are the experimental results, the solid line is the result of the full-order relativistic calculation and the dashed line is the prediction by the non-relativistic theory. The dotted lines indicate the possible alignment angles corresponding to the incoherent population of the magnetic substates.

nonrelativistic limit, where the effects of the electron spin are neglected, the total angular momentum of the final state is replaced by its orbital momentum, and the angular momentum of the emitted photon is assumed to be zero. In this situation, the orbital momentum  $\mathbf{L}_e$  of the free electron is conserved by the x-ray helicity  $|\mathbf{S}_{\text{x-ray}}| = 1$  and the orbital momentum of the final state  $|\mathbf{L}_f| = 1$ , see Fig. 6. With this configuration of the angular momenta, the alignment angle  $\gamma$  coincides with the prediction of the nonrelativistic quantum-mechanical theory, Eq. (3).

The alignment angle  $\gamma$  obtained using the nonrelativistic theory deviates from the experimental results and the predictions of the full-order relativistic theory by up to  $\approx 50^\circ$ . To interpret this, we note that the collision symmetry allows a magnetic field to be defined perpendicular to the reaction plane. Such a field is induced in the rest frame of the electron by the motion of the projectile nucleus [37,38]. Because of the spin-orbit interaction, the electron spin precesses in this field. This affects the configuration of the angular momenta before and after the collision and changes the alignment angle.

In summary, we point out that, although the photon-photon coincidence technique was used earlier [39–41], we extended it to the regime of hard x rays and to very heavy and exotic systems such as hydrogenlike uranium. This constitutes a significant experimental advancement. With

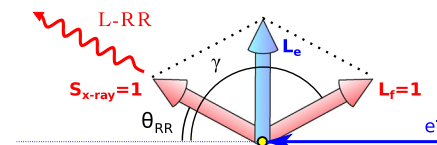


FIG. 6 (color online). Conservation of the angular momenta in RR in the nonrelativistic limit.

this technique, we, for the first time, observed the coherence between the magnetic substates in a heavy HCl. The unambiguous signature of the coherence—the tilted alignment axis, was observed through the angular distribution of the  $\text{Ly}\alpha_1$  x rays. The coherence was changed by varying the RR x-ray observation angle. The experimental results point out the strong contribution of the spin-orbit interaction to the RR process. The developed technique has a high potential for studies of alignment and polarization phenomena in various atomic processes [42]. It can also be used for diagnostics of polarized beams of heavy HCl's [43] that presently remains an unsolved problem [44].

This work was supported by the German Research Foundation (DFG) within the Emmy Noether program under Contract No. TA 740 1-1. A. S. acknowledges support from the Helmholtz Association under Contract No. VH-NG-421. A. V. M. acknowledges financial support by the Dynasty Foundation and by the grant of the President of the Russian Federation (Grant No. MK-1676.2014.2). D. B. acknowledges support from MNiSW under Grant No. NN202 463539. Y. A. L., T. S., and P.-M. H. acknowledge support by the Helmholtz-CAS Joint Research Group Contract No. HCJRG-108. The work of A. G. and C. B. was supported by the Alliance Program of the Helmholtz Association (Contract No. HA216/EMMI). We thank M. Schwemlein, K. H. Blumenhagen, T. Gassner, N. Saltybaeva, T. Habermann, D. Winters, N. Winters, R. Reuschl, as well as M. Steck and the ESR crew for their support during the beam time. We thank S. Minami for her help with electronics and J. Gerl, D. Rudolph, and B. Cederwall for lending us their detectors.

---

[1] A. Einstein, *Ann. Phys. (N.Y.)* **322**, 132 (1905).  
 [2] O. Plotzke, G. Prümper, B. Zimmermann, U. Becker, and H. Kleinpoppen, *Phys. Rev. Lett.* **77**, 2642 (1996).  
 [3] G. Snell, B. Langer, M. Drescher, N. Müller, B. Zimmermann, U. Hergenbahn, J. Viehhaus, U. Heinzmann, and U. Becker, *Phys. Rev. Lett.* **82**, 2480 (1999).  
 [4] B. A. Logan, R. Jones, A. Ljubičić, W. Dixon, and R. Storey, *Phys. Rev. A* **10**, 532 (1974).  
 [5] P. R. S. Gomes and J. Byrne, *J. Phys. B* **13**, 3975 (1980).  
 [6] S. J. Blakeway, W. Gelletly, H. R. Faust, K. Schreckenbach, and J. Byrne, *J. Phys. B* **16**, 4565 (1983).  
 [7] Th. Stöhlker *et al.*, *Phys. Rev. Lett.* **82**, 3232 (1999).  
 [8] Th. Stöhlker *et al.*, *Phys. Rev. Lett.* **86**, 983 (2001).  
 [9] S. Tashenov *et al.*, *Phys. Rev. Lett.* **97**, 223202 (2006).  
 [10] Th. Stöhlker *et al.*, *Phys. Rev. Lett.* **79**, 3270 (1997).  
 [11] A. Surzhykov, S. Fritzsche, A. Gumberidze, and Th. Stöhlker, *Phys. Rev. Lett.* **88**, 153001 (2002).  
 [12] K. Blum, *Density Matrix Theory and Applications* (Springer, New York, 2012).  
 [13] G. Weber *et al.*, *Phys. Rev. Lett.* **105**, 243002 (2010).  
 [14] P. Beiersdorfer *et al.*, *Phys. Rev. A* **53**, 3974 (1996).  
 [15] E. Takacs *et al.*, *Phys. Rev. A* **54**, 1342 (1996).

[16] D. L. Robbins, A. Faenov, T. Pikuz, H. Chen, P. Beiersdorfer, M. May, J. Dunn, K. Reed, and A. Smith, *Phys. Rev. A* **70**, 022715 (2004).  
 [17] D. L. Robbins *et al.*, *Phys. Rev. A* **74**, 022713 (2006).  
 [18] A. Gumberidze *et al.*, *Phys. Rev. Lett.* **110**, 213201 (2013).  
 [19] X. Ma, P. Mokler, F. Bosch, A. Gumberidze, C. Kozhuharov, D. Liesen, D. Sierpowski, Z. Stachura, Th. Stöhlker, and A. Warczak, *Phys. Rev. A* **68**, 042712 (2003).  
 [20] Z. Hu, X. Han, Y. Li, D. Kato, X. Tong, and N. Nakamura, *Phys. Rev. Lett.* **108**, 073002 (2012).  
 [21] S. Fritzsche, A. Surzhykov, and Th. Stöhlker, *Phys. Rev. Lett.* **103**, 113001 (2009).  
 [22] A. Surzhykov, S. Fritzsche, and Th. Stöhlker, *J. Phys. B* **35**, 3713 (2002).  
 [23] A. Maiorova, A. Surzhykov, S. Tashenov, V. M. Shabaev, S. Fritzsche, G. Plunien, and Th. Stöhlker, *J. Phys. B* **42**, 125003 (2009).  
 [24] N. Andersen, J. Gallagher, and I. V. Hertel, *Phys. Rep.* **165**, 1 (1988).  
 [25] N. Andersen and K. Bartschat, *Polarization, Alignment, and Orientation in Atomic Collisions* (Springer, New York, 2001).  
 [26] K. Bartschat, *Phys. Rep.* **180**, 1 (1989).  
 [27] A. Raeker, K. Blum, and K. Bartschat, *J. Phys. B* **26**, 1491 (1993).  
 [28] V. V. Balashov, A. N. Grum-Grzhimailo, and N. M. Kabachnik, *Polarization and Correlation Phenomena in Atomic Collisions A Practical Theory Course* (Kluwer Academic, New York, 2000).  
 [29] B. Franzke, *Nucl. Instrum. Methods Phys. Res., Sect. B* **24–25**, 18 (1987).  
 [30] J. Eichler and Th. Stöhlker, *Phys. Rep.* **439**, 1 (2007).  
 [31] Th. Stöhlker *et al.*, *Phys. Rev. A* **51**, 2098 (1995).  
 [32] G. Duchêne, F. A. Beck, P. J. Twin, G. de France, D. Curien, L. Han, C. W. Beausang, M. A. Bentley, P. J. Nolan, and J. Simpson, *Nucl. Instrum. Methods Phys. Res., Sect. A* **432**, 90 (1999).  
 [33] S. L. Shepherd *et al.*, *Nucl. Instrum. Methods Phys. Res., Sect. A* **434**, 373 (1999).  
 [34] J. Eberth, H. G. Thomas, P. V. Brentano, R. M. Lieder, H. M. Jäger, H. Kämmerling, M. Berst, D. Gutknecht, and R. Henck, *Nucl. Instrum. Methods Phys. Res., Sect. A* **369**, 135 (1996).  
 [35] A. Georgiev, W. Gast, and R. M. Lieder, *IEEE Trans. Nucl. Sci.* **41**, 1116 (1994).  
 [36] N. M. Kabachnik and K. Ueda, *J. Phys. B* **28**, 5013 (1995).  
 [37] S. Tashenov, T. Bäck, R. Barday, B. Cederwall, J. Enders, A. Khaplanov, Yu. Poltoratska, K.-U. Schässburger, and A. Surzhykov, *Phys. Rev. Lett.* **107**, 173201 (2011).  
 [38] S. Tashenov *et al.*, *Phys. Rev. A* **87**, 022707 (2013).  
 [39] R. Ali *et al.*, *Phys. Rev. A* **55**, 994 (1997).  
 [40] H. W. Schäffer, R. Dunford, E. Kanter, S. Cheng, L. Curtis, A. Livingston, and P. Mokler, *Phys. Rev. A* **59**, 245 (1999).  
 [41] Z. Hu, Y. Li, A. Yamazaki, and N. Nakamura, *Phys. Scr.* **T144**, 014047 (2011).  
 [42] A. V. Maiorova, A. Surzhykov, S. Tashenov, V. M. Shabaev, and Th. Stöhlker, *Phys. Rev. A* **86**, 032701 (2012).  
 [43] A. Surzhykov, S. Fritzsche, and Th. Stöhlker, *Nucl. Instrum. Methods Phys. Res., Sect. B* **205**, 391 (2003).  
 [44] A. Bondarevskaya, A. Prozorov, L. Labzowsky, G. Plunien, D. Liesen, and F. Bosch, *Phys. Rep.* **507**, 1 (2011).